

1 **Title:** Temperature-mediated changes in microbial carbon use efficiency and <sup>13</sup>C discrimination

2

3 **Author list and affiliations:**

4 Christoph A. Lehmeier<sup>1</sup>, Ford Ballantyne IV<sup>1,2</sup>, Kyungjin Min<sup>1</sup>, Sharon A. Billings<sup>1\*</sup>

5 <sup>1</sup>Department of Ecology and Evolutionary Biology, Kansas Biological Survey, University of  
6 Kansas, 2101 Constant Ave., Lawrence, KS 66047, USA.

7 <sup>2</sup>now: Odum School of Ecology, University of Georgia, 140 E. Green St., Athens, GA 30602,  
8 USA.

9 **\*Corresponding author:**

10 Sharon A. Billings, Kansas Biological Survey, University of Kansas, 2101 Constant Ave.,  
11 Lawrence, KS 66047, USA. Tel.: 001-785-864-1560, Fax: 001-785-864-1534, email:

12 [Sharon.Billings@ku.edu](mailto:Sharon.Billings@ku.edu)

13

14

15

16

17

18

19 **Abstract**

20 Understanding how carbon dioxide (CO<sub>2</sub>) flux from ecosystems feeds back to climate warming  
21 depends in part on our ability to quantify the efficiency with which microorganisms convert  
22 organic carbon (C) into either biomass or CO<sub>2</sub>. Quantifying ecosystem-level respiratory CO<sub>2</sub>  
23 losses often also requires assumptions about stable C isotope fractionations associated with the  
24 microbial transformation of organic substrates. However, the diversity of organic substrates'  
25  $\delta^{13}\text{C}$  and the challenges of measuring microbial C use efficiency (CUE) in their natural  
26 environment fundamentally limit our ability to project ecosystem C budgets in a warming  
27 climate. Here, we quantify the effect of temperature on C fluxes during metabolic  
28 transformations of cellobiose, a common microbial substrate, by a cosmopolitan microorganism  
29 growing at a constant rate. Biomass-C specific respiration rate increased by 250% between 13  
30 °C and 26.5 °C, decreasing CUE from 77% to 56%. Biomass-C specific respiration rate was  
31 positively correlated with an increase in respiratory <sup>13</sup>C discrimination from 4.4‰ to 6.7‰  
32 across the same temperature range. This first demonstration of a direct link between  
33 temperature, microbial CUE and associated isotope fluxes provides a critical step towards  
34 understanding  $\delta^{13}\text{C}$  of respired CO<sub>2</sub> at multiple scales, and towards a framework for predicting  
35 future ecosystem C fluxes.

36

37 **1 Introduction**

38 Because Earth's C cycle is a key regulator of climate, a central goal of biogeochemistry is to  
39 understand biosphere-atmosphere C exchange. Globally, almost all C initially assimilated via

40 photosynthesis is respired back to the atmosphere as CO<sub>2</sub> by auto- and heterotrophic organisms  
41 (Schimel, 1995; Trumbore, 2006). Though we have a reasonably comprehensive understanding  
42 of how environmental conditions influence CO<sub>2</sub> uptake by photosynthetic organisms, our  
43 understanding of how respiratory CO<sub>2</sub> fluxes respond to environmental conditions significantly  
44 lags behind. This is especially true for respiratory CO<sub>2</sub> derived from heterotrophs, which may  
45 account for more than half of respiratory C losses from soils and aquatic systems (Kucera and  
46 Kirkham, 1971; Hanson et al., 2000; Cotner and Biddanda, 2002; Subke et al., 2006). Metabolic  
47 rates of heterotrophs are expected to increase with rising temperatures (Gillooly et al., 2001;  
48 Pomeroy and Wiebe, 2001; Hall et al., 2008), which is of great concern given Earth's large  
49 reservoir of reduced organic matter (OM) that may be mineralized to CO<sub>2</sub> via metabolism  
50 (Hedges et al., 2000; Kirschbaum, 2006). The influence of temperature on the physiology of  
51 heterotrophic microbes must therefore be well understood to project shifts in the global C  
52 balance in a warmer climate.

53 Existing knowledge of Earth's terrestrial C balance has been bolstered by the use of stable  
54 isotopes. A milestone for progress was when photosynthetic responses to environmental  
55 conditions were linked to differences between the stable C isotopic composition ( $\delta^{13}\text{C}$ ) of  
56 atmospheric CO<sub>2</sub> and that of plant products (Farquhar et al., 1982). These differences, caused by  
57 C isotope fractionation during CO<sub>2</sub> diffusion into leaves and subsequent carboxylation (Park and  
58 Epstein, 1961; O'Leary, 1981), impart an isotopic fingerprint on ecosystem C pools and permit  
59 inference about C fluxes from  $\delta^{13}\text{C}$  of ecosystem C pools at multiple spatio-temporal scales  
60 (Farquhar and Richards, 1984; Pataki et al., 2003; Dijkstra et al., 2004; Barbosa et al., 2010).  
61 Recent studies remind us that respiratory C losses also leave an isotopic fingerprint on  $\delta^{13}\text{C}$   
62 values of plant tissues via respiration of substrates with distinct  $\delta^{13}\text{C}$  (Bathellier et al., 2009;

63 Brüggemann et al. 2011; Ghashghaie and Badeck, 2014), and via C isotope fractionation during  
64 decarboxylation in respiratory pathways (Werner and Gessler, 2011; Werner et al., 2011;  
65 Tcherkez et al., 2012). Though not all C isotope fractionations during metabolism are well-  
66 characterized,  $\delta^{13}\text{C}$  of metabolic reaction substrates and products can vary predictably, caused by  
67 kinetic or thermodynamic isotope effects (Rossmann et al., 1991; Gleixner and Schmidt, 1997;  
68 Cleland, 2005; Tcherkez et al., 2012). Accounting for isotope effects in plant respiratory C  
69 losses improves our ability to quantify the contributions of different pools to  $\text{CO}_2$  fluxes and thus  
70 our predictions of terrestrial ecosystem C budgets under changing environmental conditions.  
71 Using  $\delta^{13}\text{C}$  of heterotrophically respired  $\text{CO}_2$  holds similar promise, but if and how changing  
72 environmental conditions influence any fractionation factors for the fluxes associated with the  
73 liberation of C from OM is unknown.

74 Significant uncertainty about the direction and magnitude of C isotope fractionation during  
75 microbial C transformations (Bowling et al., 2008; Werth and Kuzyakov, 2010) renders  
76 quantifying microbial  $\text{CO}_2$  fluxes in ecosystems difficult. Difficulties arise because microbes in  
77 natural systems can access a diverse array of organic substrates with distinct  $\delta^{13}\text{C}$  signatures  
78 (Park and Epstein, 1961; Billings, 2006), the respiration of which influences  $\delta^{13}\text{C}$  of respired  
79  $\text{CO}_2$ . Though we know the growth rate of microbial populations influences C flux into and  
80 through biomass (Kayser et al., 2005), it is impossible to directly quantify microbial growth *in*  
81 *situ*. Furthermore, absence of steady state conditions over a course of  $\text{CO}_2$  flux measurements  
82 makes the interpretation of temperature effects on the magnitude and the  $\delta^{13}\text{C}$  of ecosystem  
83 respiration an even greater challenge (Gamnitzer et al., 2011; Nickerson et al., 2013). Thus,  
84 establishing a mechanistic understanding of the links between temperature, microbial respiration  
85 rates and C isotope fractionation during substrate transformations at a fundamental level requires

86 that we characterize these processes as temperature changes in isolation from other factors that  
87 influence microbial C transformations.

88 To assess the influence of temperature on microbial growth and respiration rates, we grew a  
89 widely distributed Gram-negative, heterotrophic bacterium (*Pseudomonas fluorescens*) in  
90 continuous culture bioreactors (chemostats) at seven temperatures ranging from 13 °C to 26 °C  
91 (Fig. 1) at reactor dilution rates of approximately 0.14 h<sup>-1</sup>, which is equivalent to the relative  
92 growth rates of the microbial populations (Dawson, 1974; Smith and Waltman, 1995; Goldman  
93 and Dennett, 2000; Chrzanowski and Grover, 2008; Ferenci, 2008; Bull, 2010; Egli, 2015). We  
94 measured microbial respiration rates and  $\delta^{13}\text{C}$  of respired CO<sub>2</sub> in this open, flow-through system  
95 at steady-state (Craig and Gordon, 1965; Fry, 2006; see Supplementary Material for a detailed  
96 elaboration of this approach). We computed the temperature dependence of a widely applied  
97 metric of microbial C use efficiency (CUE), defined as  $\text{SGR} / (\text{SGR} + \text{SRR})$ , where SGR and SRR  
98 are specific growth and specific respiration rates respectively, with units of C per microbial  
99 biomass-C and time. Our simplified system has several assets. First, it eliminates factors present  
100 in natural environments that preclude accurate assessment of specific growth and respiration  
101 rates, and thus accurate estimates of CUE as defined above. Second, obtaining accurate  
102 estimates of microbial CUE is critical for projecting C fluxes into the future because the  
103 particular value of CUE significantly influences CO<sub>2</sub> loss rates from ecosystems in models of  
104 OM decomposition (Allison et al., 2010; Wieder et al., 2013). Finally, simultaneously  
105 quantifying differences in  $\delta^{13}\text{C}$  of organic substrate, microbial biomass-C and respired CO<sub>2</sub> along  
106 a temperature gradient is critical for partitioning synoptic CO<sub>2</sub> measurements into component  
107 fluxes.

108

## 109 **2 Materials and Methods**

### 110 **2.1 Pre-cultivation of microorganisms for chemostat inoculation**

111 We pre-cultivated *Pseudomonas fluorescens* (Carolina Biological Supply, USA) in nutrient  
112 solution containing 10 mM NH<sub>4</sub>Cl, 1.6 mM KNO<sub>3</sub>, 2.6 mM K<sub>2</sub>HPO<sub>4</sub>, 1.0 mM KH<sub>2</sub>PO<sub>4</sub>, 0.8 mM  
113 MgSO<sub>4</sub>, 0.2 mM CaCl<sub>2</sub>, 0.1 mM CuCl<sub>2</sub>, 0.04 mM FeSO<sub>4</sub>, 0.03 mM MnCl<sub>2</sub> and 0.02 mM ZnSO<sub>4</sub>,  
114 modified from Abraham et al. (1998). The sole C source in the nutrient medium was 10 mM  
115 cellobiose (C<sub>12</sub>H<sub>22</sub>O<sub>11</sub>; with a δ<sup>13</sup>C of -24.2‰); cellobiose is a disaccharide consisting of two  
116 glucose molecules and a basic module of cellulose. Thus, the C to N to P atomic ratio of the  
117 autoclaved, sterile nutrient solution was 100 to 10 to 3.3; its pH was adjusted to 6.5. The  
118 bacteria grew for a few days in batch culture in a flask fitted with a vent for air exchange covered  
119 by a 0.22 µm filter (Fisher Scientific, USA) to avoid contamination. Vessel contents were stirred  
120 continuously in an incubator maintained at 10 °C.

### 121 **2.2 The laboratory mesocosm – the chemostat**

122 The chemostat system was composed of two 1.9 L vessels, a medium reservoir tank and a  
123 reactor, each maintained on separate heating/stirring plates (Fig. 1) in separate incubators. The  
124 reactor volume was on average 870 mL (Supplementary Table 1). The reservoir tank was  
125 connected via a flexible tube to the reactor (Tygon E-LFL pump tubing, Masterflex, USA),  
126 which in turn had an outlet tube (Fig. 1; both tubes had a 1.6 mm inner diameter). When the  
127 chemostat was operated in “continuous culture mode” a peristaltic pump transported fresh  
128 medium to the reactor and simultaneously removed medium from the reactor at the same rate.

129 Thus, reactor volume remained constant during all chemostat runs. The 0.22  $\mu\text{m}$  filter in the  
130 reservoir tank lid allowed for pressure compensation during withdrawal of nutrient solution in  
131 the continuous flow mode. Experimental temperatures were continuously measured with a  
132 thermometer (Oakton, USA) placed in the reactor medium (Fig. 1). This thermometer was  
133 routinely compared against an internal laboratory standard mercury thermometer, before and at  
134 the end of each experiment. The reactor temperatures were adjusted with heating/stirring plate  
135 and incubator settings, and kept constant during all experimental runs.

136 The reactor lid had two ports for gas lines. The outlet port tube was connected to a  $^{13}\text{CO}_2/^{12}\text{CO}_2$   
137 analyzer (G2101-i, Picarro, USA) containing a pump that continuously removed air from the  
138 reactor headspace at an average rate of  $0.025 \text{ L min}^{-1}$ . A water trap (magnesium perchlorate,  
139 Costech, USA) was installed between outlet port of the reactor and the gas analyzer. The  $\text{CO}_2$   
140 analyzer recorded the concentration and the  $\delta^{13}\text{C}$  of the reactor headspace  $\text{CO}_2$  at 0.5 Hz. The  
141 reactor's inlet tube was connected to a mass flow controller (MC-50SCCM, Alicat Scientific,  
142 USA), which in turn, was connected to a gas cylinder containing  $\text{CO}_2$ -free air (Fig. 1). The mass  
143 flow controller was programmed to maintain the reactor headspace at constant atmospheric  
144 pressure; thus, the  $0.025 \text{ L min}^{-1}$  headspace air removed by the  $^{13}\text{CO}_2/^{12}\text{CO}_2$  analyzer pump was  
145 instantaneously replaced with  $\text{CO}_2$ -free air flowing from the gas cylinder into the reactor  
146 medium. Assuming (1) that 1 mol of  $\text{O}_2$  is consumed per 1 mol of  $\text{CO}_2$  produced in aerobic  
147 respiration, (2) a typical reactor headspace  $\text{CO}_2$  concentration of around 2000 ppm at steady state  
148 (see Fig. 2A and below), and (3) an  $\text{O}_2$  concentration of 21% in the air supply to the reactor, the  
149 air supply permitted continuous aerobic metabolism. Routine tests with  $\text{CO}_2$ -free air in sterile  
150 chemostats were performed to ensure there were no leaks in the system.

### 151 **2.3. The chemostat run – standardized protocol and description of events**

152 We conducted seven independent chemostat runs, at temperatures of 13, 14.5, 16, 18, 21, 23.5  
153 and 26.5 °C at a dilution rate of, on average,  $0.14 \text{ h}^{-1}$ , in random temporal order. For each of the  
154 chemostat runs, we inoculated the reactor with a 10 mL aliquot of the *P. fluorescens* pre-culture  
155 and activated the flow of CO<sub>2</sub>-free air through the reactor; this was considered time 0. At the  
156 initial stage of a chemostat run, the bacteria grew in batch culture, that is, there was no flow of  
157 fresh nutrient medium from the reservoir tank to the reactor, and no removal of medium from the  
158 reactor (Fig. 1).

#### 159 **2.3.1 Respiration measurements at chemical and isotopic equilibrium in the continuous** 160 **flow chemostat at steady-state**

161 At the initial pH of 6.5, inorganic C in the fresh reactor medium was mainly in the form of  
162 H<sub>2</sub>CO<sub>3</sub> (aq) and HCO<sub>3</sub><sup>-</sup> (Stumm and Morgan, 1981). By continuously bubbling CO<sub>2</sub>-free air into  
163 the reactor, we expelled these initial inorganic C pools from the reactor medium. This was  
164 evident by concentrations of reactor headspace CO<sub>2</sub> of virtually zero in the early stages of batch  
165 culture after each run's inoculation (Fig. 2A). During the phase of rising reactor headspace CO<sub>2</sub>  
166 via respiratory activity of the exponentially growing population (Fig. 2A), inorganic C in the  
167 reactor medium accrued with the increasing addition of CO<sub>2</sub> from microbial respiration. That is,  
168 at any point in time during the phase of increasing reactor headspace CO<sub>2</sub> concentration, the  
169 nutrient medium acted as a sink for respired CO<sub>2</sub> (see also Supplementary Material).

170 Once the respiratory activity of the growing microbial population pushed the reactor headspace  
171 CO<sub>2</sub> concentration above 500 ppm, we transferred the chemostat into the “continuous culture,



172 open system” mode (Figs. 1, 2; Ferenci, 2008; Bull, 2010). The peristaltic pump henceforth  
173 transported fresh nutrient medium from the reservoir tank to the reactor at a constant rate of, on  
174 average, 118 mL h<sup>-1</sup> (Supplementary Table 1), and simultaneously removed medium from the  
175 reactor at the same rate so that the reactor volume remained constant. Initial chemostat  
176 experiments indicated that when headspace CO<sub>2</sub> concentrations reached 500 ppm, the bacterial  
177 population was sufficiently dense to maintain itself without being washed out via dilution.  
178 Depending on the reactor temperature, the onset of the continuous culture mode occurred  
179 between 40 h (at 26.5 °C) and 72 h (at 13 °C) after inoculation.

180 After the switch from batch to continuous culture, the rate of increase in reactor headspace CO<sub>2</sub>  
181 concentration gradually slowed because cells were continuously diluted into the waste stream  
182 (Fig. 1), and approached a phase where the CO<sub>2</sub> concentration became stable (Fig. 2A). At this  
183 point, bacteria grown in continuous culture had reached the phase of steady-state growth and  
184 physiology (see Ferenci, 2008; Bull, 2010). A key feature of the continuous culture chemostat  
185 relevant to our study is that at this steady-state, the constant dilution rate of the reactor (the  
186 medium flow rate divided by the reactor volume) is equivalent to the specific growth rate of the  
187 microbial culture (Bull, 2010). That is, washout of cells with the nutrient medium flow is  
188 balanced by cell division so that the size of the population in the reactor can be expected to be  
189 reasonably constant in the time frames employed here (see discussion in Ferenci, 2008; Bull,  
190 2010).

191 Critically, when reactor headspace CO<sub>2</sub> concentrations approached the steady-state, inorganic C  
192 pools came to their respective equilibria as well (Stumm and Morgan, 1981). At this point, pools  
193 of H<sub>2</sub>CO<sub>3</sub> (aq) and HCO<sub>3</sub><sup>-</sup> were no longer a *net* sink for respired CO<sub>2</sub>. As reactor headspace CO<sub>2</sub>

194 concentrations reached steady state, the system supported constant microbial CO<sub>2</sub> production  
195 reflective of steady-state growth under constant environmental conditions, and reflected  
196 chemical equilibrium (i.e., constant size) of the dissolved inorganic C pools. Thus, the rate of  
197 CO<sub>2</sub> addition to the reactor headspace volume at steady-state accurately represented the CO<sub>2</sub>  
198 released during microbial respiration (see also Supplementary Material).

199 We calculated the molar CO<sub>2</sub> production rate of the microbial population as the product of the  
200 average molar CO<sub>2</sub> concentration measured by the <sup>13</sup>CO<sub>2</sub>/<sup>12</sup>CO<sub>2</sub> analyzer for 5 hours at steady  
201 state (Fig. 2A) multiplied by the molar air flow rate through the reactor, which was calculated as

202 
$$\text{Air flow (mol min}^{-1}\text{)} = 0.96 \text{ atm} * 0.025 \text{ L min}^{-1} / (0.082 \text{ atm L mol}^{-1} \text{ K}^{-1} * 296 \text{ K}),$$

203 with 0.96 atm and 296 K being the barometric pressure and the temperature in the lab where the  
204 experiments were performed, 0.025 L min<sup>-1</sup> the average volumetric headspace flow rate through  
205 the reactor and 0.082 atm L mol<sup>-1</sup> K<sup>-1</sup> the gas constant.

206 The δ<sup>13</sup>C of the reactor headspace CO<sub>2</sub> during the earliest batch culture phase was generally very  
207 negative; the <sup>13</sup>CO<sub>2</sub>/<sup>12</sup>CO<sub>2</sub> analyzer cannot accurately measure <sup>13</sup>C and <sup>12</sup>C in very low CO<sub>2</sub>  
208 concentrations (Fig. 2B). The δ<sup>13</sup>C of reactor headspace CO<sub>2</sub> became less negative as the CO<sub>2</sub>  
209 concentration increased (Fig. 2B). During the “climbing” phase of the reactor headspace CO<sub>2</sub>,  
210 the δ<sup>13</sup>C of the CO<sub>2</sub> pool was influenced by isotopic fractionation among gaseous CO<sub>2</sub>, H<sub>2</sub>CO<sub>3</sub>  
211 (aq) and HCO<sub>3</sub><sup>-</sup> (Vogel et al., 1970; Mook et al., 1974; Stumm and Morgan, 1981; Szaran, 1997),  
212 because the dissolved inorganic C pools functioned as a net sink for respired CO<sub>2</sub>. At steady-  
213 state, with constant headspace CO<sub>2</sub> concentrations and constant size of the dissolved inorganic C  
214 pools (see above), isotopic equilibrium was achieved, evidenced by constant δ<sup>13</sup>C readings of

215 reactor headspace CO<sub>2</sub> (Fig. 2B). As such, in this open system at steady-state, the  $\delta^{13}\text{C}$  of the  
216 CO<sub>2</sub> leaving the reactor (the CO<sub>2</sub> measured by the analyzer) is identical to the  $\delta^{13}\text{C}$  of microbial  
217 respiration (Craig and Gordon, 1965; Fry, 2006). Importantly, this principle is valid irrespective  
218 of temperature, microbial growth rate or microbial biomass in the reactor. (See Supplementary  
219 Material for an elaboration of the principle of chemical and isotopic equilibrium.)

220 We used the average  $\delta^{13}\text{C}$  measurement of reactor headspace CO<sub>2</sub> over the same five hours in the  
221 stable phase employed for calculations of microbial respiration rates (see above) as the isotopic  
222 signature of CO<sub>2</sub> respired by the microbial culture at each temperature. Any measurements of  
223 headspace CO<sub>2</sub> and  $\delta^{13}\text{C}$  during the climbing phase before steady-state (Fig. 2) were not used in  
224 these calculations.

225 For the example chemostat at 23.5 °C, the half-life of the reactor ( $t_{1/2}$ ), i.e., the time it took until  
226 50% of the reactor medium was exchanged with fresh tank medium, was 5.2 h (with  $t_{1/2} = \ln(2) /$   
227 (medium flow rate / reactor volume); Supplementary Table 1). In a homogeneous, well-mixed  
228 system such as that employed here, 95% of the pool (i.e., the reactor) is exchanged with new  
229 medium within approximately five times the half-life. Thus, during the respiration  
230 measurements between time 70 h and 74 h (in the example time course in Fig. 2), any “leftovers”  
231 from the batch culture mode were insignificant, and the microbial culture could be considered  
232 homogeneous. This principle was applicable to all chemostat runs we performed.

233 After the 5-hour respiration measurements were completed, we disconnected the gas lines from  
234 the reactor, connected the mass flow controller directly to the <sup>13</sup>CO<sub>2</sub>/<sup>12</sup>CO<sub>2</sub> analyzer, and replaced  
235 the CO<sub>2</sub>-free air cylinder with a reference gas cylinder containing 1015 ppm CO<sub>2</sub> at a  $\delta^{13}\text{C}$  of -  
236 48.9‰ (Matheson, USA). This laboratory standard gas was previously calibrated against

237 secondary CO<sub>2</sub> standards (Oztech, USA) and served for any necessary corrections of the  $\delta^{13}\text{C}$  of  
238 the reactor headspace CO<sub>2</sub> measurements. Across the seven standard measurement procedures  
239 after each individual chemostat run, the  $\delta^{13}\text{C}$  measured for the laboratory standard gas showed  
240 only slight variation (1 SD = 0.16‰). CO<sub>2</sub> concentration measurements needed no correction;  
241 measurements of lab-internal gases with previously determined CO<sub>2</sub> concentrations between  
242 chemostat runs showed very stable and accurate analyzer performance.

### 243 **2.3.2 Measurements of extracellular enzyme activities at steady-state**

244 Using principles detailed by Lehmeier et al. (2013) and Min et al. (2014), we tested reactor  
245 medium for activity of the extracellular enzymes  $\beta$ -glucosidase and  $\beta$ -N-acetyl glucosaminidase  
246 across all chemostat temperatures; we never detected extracellular activity of either enzyme. The  
247 lack of extracellular  $\beta$ -glucosidase activity indicates that the sole C source, cellobiose, was  
248 directly taken up by microbes and cleaved intracellularly into glucose monomers for further  
249 metabolism. The lack of extracellular  $\beta$ -N-acetyl glucosaminidase activity suggests that the  
250 inorganic N provided in nutrient medium was the sole source of N taken up by *P. fluorescens*.  
251 These findings do not rule out the possibility that *P. fluorescens* may have taken up (i.e. recycled)  
252 any exuded C-based metabolic compounds, although such a scenario in continuous culture  
253 conditions may not appear to be energetically favorable. Thus, the assumption that the sole  
254 resources used by *P. fluorescens* were the cellobiose and the nutrient medium appears reasonable.

### 255 **2.3.3 Harvest of microbial biomass at steady-state**

256 Immediately after completing the 5 hour respiration measurements, we filtered approximately  
257 300 mL of reactor medium for steady-state microbial biomass using 0.2  $\mu\text{m}$  filters made of

258 polyethersulfone (Pall, USA) and a vacuum pump. The filters had previously been oven-dried  
259 for 48 h at 75 °C and their dry weight determined. We then oven-dried the filters post filtration  
260 for 48 h at 75 °C, removed some of the dry biomass and weighed 1.2 mg of the material into tin  
261 cups for subsequent combustion in an elemental analyzer (1110 CHN Combustion Analyzer,  
262 Carlo Erba Strumentazione, Italy) coupled to a ThermoFinnigan DeltaPlus mass spectrometer  
263 (Finnigan MAT, Germany) at the Keck Paleoenvironmental and Environmental Stable Isotope  
264 Laboratory (The University of Kansas, USA). We thus determined biomass C (and N) elemental  
265 content, as well as the  $\delta^{13}\text{C}$  of the biomass. In this analysis, the samples were compared against  
266 a laboratory standard  $\text{CO}_2$  previously calibrated against the same secondary  $\text{CO}_2$  standards as  
267 used in calibration of the  $\text{CO}_2$  standard used for respiration measurements (see above). The  $\delta^{13}\text{C}$   
268 of the substrate cellobiose was measured likewise. Dry weight of the sampled reactor aliquots  
269 and the C content obtained from elemental analysis served to calculate total microbial C content  
270 in the steady-state reactor and to calculate specific respiration rates.

271 At all temperatures studied, biomass C and N contents were virtually the same, on average 27%  
272 and 8% of microbial dry mass, respectively (Supplementary Table 1). From mass balance  
273 calculations, we determined that only a small percentage of the C and N supplied via fresh  
274 medium from the tank was taken up to fuel microbial growth (2.8 % and 4.3 % on average for C  
275 and N, respectively). This suggests that the observed temperature effects on specific respiration  
276 rates and CUE were not confounded by any differences in C and N limitations at the different  
277 temperatures (Goldmann and Denner, 2000; Cotner et al., 2006; Chrzanowski and Grover, 2008).

278

### 279 **3 Results and Discussion**

280 For *P. fluorescens* grown in continuous culture, CUE, defined as  $SGR / (SGR + SRR)$ , declined  
281 with increasing temperature, from 77% at 13 °C to 56% at 26.5 °C (Fig. 3A). Because specific  
282 growth rates were similar across the experimental temperatures ( $137 \text{ mg g}^{-1} \text{ h}^{-1}$ ,  $\pm 8$  (1 SD); or  
283  $13.7 \% \text{ h}^{-1}$  in relative terms; Fig. 3B), the decline in CUE was due to the 2.5 fold increase of SRR  
284 with temperature, which rose from  $45 \text{ mg g}^{-1} \text{ h}^{-1}$  at 13 °C to  $113 \text{ mg g}^{-1} \text{ h}^{-1}$  at 26.5 °C (Fig. 3B).  
285 The decline in CUE is also evident in the more than 50% reduction in steady-state dry microbial  
286 biomass with increasing temperature (Fig. 3A). For example, though SGR was approximately  
287 the same and thus the fraction of biomass replaced per time similar across all experimental  
288 temperatures (0.147 and 0.141 at 13 °C and 26.5 °C, respectively; Fig. 3B) microbes at 13 °C  
289 generated  $20.9 \text{ mg biomass h}^{-1}$  while those at 26.5 °C generated less than half the amount ( $9.5$   
290  $\text{ mg biomass h}^{-1}$ ).

291 Because we did not quantify possible C losses from the population at steady-state such as  
292 secretion of organic acids or other compounds (El-Mansi and Holms, 1989; Nanchen et al.,  
293 2006), gross rates of steady-state cellobiose C uptake may have been slightly higher than what  
294 was calculated from the sum of SGR and SRR. However, the direct observation of *P.*  
295 *fluorescens*' CUE is consistent with the negative effect of increasing temperature on microbial  
296 CUE widely reported in literature for soils and aquatic ecosystems (del Giorgio and Cole, 1998;  
297 Gillooly et al., 2001; Rivkin and Legendre, 2001; Apple et al., 2006; Manzoni et al., 2012; Frey  
298 et al., 2013; Tucker et al., 2013).

299 Across the chemostat runs, we observed strong C isotope fractionations, which created  
300 pronounced differences in  $\delta^{13}\text{C}$  between microbial biomass and the sole C substrate, cellobiose,  
301 and between microbial biomass and respired  $\text{CO}_2$  (Fig. 4). Microbial biomass exhibited 5.5 to

302 10.5‰ more negative  $\delta^{13}\text{C}$  values than the cellobiose and respired  $\text{CO}_2$  was even more  $^{13}\text{C}$   
303 depleted, at least 4.4‰ more negative than the biomass (Fig. 4A). Because each chemostat was  
304 at steady-state, isotopic mass balance dictates that  $^{13}\text{C}$  “missing” from cellobiose had to  
305 accumulate in another pool in the reactor. The only pool that could have been enriched with the  
306 “missing”  $^{13}\text{C}$  was reactor DOC, which we analyzed for  $\delta^{13}\text{C}$  in four out of the seven chemostat  
307 runs (Fig. 4A). Reactor DOC consisted of a large pool of cellobiose (because the rate of C  
308 consumption by the chemostat cultures was, on average, only 2.8% of the rate of C supply) and  
309 presumably a pool of additional organic compounds (e.g. acetate). Such compounds appear to be  
310 typically secreted from microbial cells at low rates in aerobic chemostats operated at dilution  
311 rates similar to those of our runs (El-Mansi and Holms, 1989; Nanchen et al., 2006), and have  
312 been shown to be enriched in  $^{13}\text{C}$  compared to cellular biomass (Blair et al., 1985). However,  
313 because such a small fraction of the available cellobiose was taken up by *P. fluorescens*, the  
314 fraction of total DOC comprised of secreted organic compounds was small. As a result,  $^{13}\text{C}$   
315 enrichment of any microbial exudates was insufficient to enrich bulk DOC to an extent  
316 detectable by the isotope-ratio mass spectrometer (Fig. 4A).

317 The majority of the fractionation between *P. fluorescens* biomass and the substrate was most  
318 likely due to discrimination against  $^{13}\text{C}$  during cellobiose uptake. If we assume that *P.*  
319 *fluorescens* secreted organic compounds at a rate of 10% of the sum of SGR and SRR (El-Mansi  
320 and Holms, 1989) and that the bacteria did not discriminate against  $^{13}\text{C}$ -containing cellobiose  
321 during uptake (and thus assimilated cellobiose possessed a  $\delta^{13}\text{C}$  of -24.2‰), isotopic mass  
322 balance dictates that the  $\delta^{13}\text{C}$  of the C secretion flux (Fig. 5) would have to be +70‰, at  
323 minimum, across all temperatures. To our knowledge, such high metabolic discrimination  
324 against  $^{13}\text{C}$  would be very unusual for biological systems (O’Leary, 1981). An alternative and

325 more likely scenario is therefore that *P. fluorescens* took up less  $^{13}\text{C}$ -containing cellobiose than  
326 was supplied as substrate, and that discrimination during uptake contributed substantially to *P.*  
327 *fluorescens* biomass and respired  $\text{CO}_2$  being more  $^{13}\text{C}$  depleted than the cellobiose supplied.  
328 This conclusion holds for all temperatures studied. If we assume for the example  $23.5\text{ }^\circ\text{C}$   
329 chemostat run at steady-state (Figs. 2, 5) that *P. fluorescens* secreted organic compounds at a rate  
330 of 10% of the sum of SGR and SRR, and we further assume that the  $\delta^{13}\text{C}$  of secreted compounds  
331 was 11.7‰ less negative than that of the biomass (Blair et al., 1985), that is -18.1‰, then the  
332  $\delta^{13}\text{C}$  of the cellobiose taken up would have been -31.1‰, which is only a 7‰ difference from the  
333 cellobiose provided, and therefore probably a more likely scenario (Fig. 5).

334 Substantial  $^{13}\text{C}$  depletion of respired  $\text{CO}_2$  relative to microbial biomass has not, to our  
335 knowledge, been reported in other studies. With the microbial C consumption rate amounting to  
336 only 2.8% of the rate of C supply, C availability was high compared to what microbes in their  
337 natural environments typically experience (Tempest and Neijssel, 1978; Cole et al., 1988;  
338 Hobbie and Hobbie, 2013), potentially promoting enzymatic discrimination. The cellobiose  $\delta^{13}\text{C}$   
339 of -24.2 ‰ implies a  $^{13}\text{C}/^{12}\text{C}$  ratio of  $\sim 1/91$ . Considering the molecular formula of cellobiose  
340  $\text{C}_{12}\text{H}_{22}\text{O}_{11}$ , this means that not more than about one out of eight cellobiose molecules in the  
341 supplied substrate included a  $^{13}\text{C}$  atom. Faster diffusion of the isotopically lighter cellobiose  
342 molecules may have contributed to a lower probability of  $^{13}\text{C}$ -containing cellobiose approaching  
343 bacterial membrane uptake sites, and hence, to the differences between  $\delta^{13}\text{C}$  of substrate and  
344 biomass (Fig. 4A). However, isotope fractionation during diffusion – a physical process  
345 dependent on compound mass – would likely exhibit a continuous temperature response. Thus,  
346 it seems unlikely that fractionation during diffusion was the primary driver of the pronounced,  
347 discontinuous changes in the difference between substrate and biomass  $\delta^{13}\text{C}$ , which ranged from



348 5.5 to 10.5‰ (Fig. 4A). Rather, this variation, with one apparently linear part between 13 °C and  
349 16 °C and another between 18 °C and 23.5 °C, may be explained parsimoniously by a  
350 significant, discontinuous reorganization of enzyme-mediated C fluxes into and out of bacterial  
351 cells (see Nanchen et al., 2006), induced by differences in temperature at which *P. fluorescens*  
352 was growing and the related differences in substrate uptake rates.

353 Evidence from work on C isotope distribution within carbohydrate molecules (e.g., Rossmann et  
354 al., 1991; Gleixner and Schmidt, 1997) suggests non-random distribution of <sup>13</sup>C in biological  
355 molecules (such as cellobiose). Based on such phenomena, it is probable that the <sup>13</sup>C atom in  
356 <sup>13</sup>C-containing cellobiose was consistently at the same position within the molecule, which rules  
357 out the possibility that any changes in the intramolecular <sup>13</sup>C distribution of cellobiose were  
358 responsible for the observed  $\delta^{13}\text{C}$  patterns in biomass and respired CO<sub>2</sub> (Fig. 4). Hence, the  
359 discontinuous pattern of  $\delta^{13}\text{C}$  of respired CO<sub>2</sub> with temperature, similar to the pattern for  $\delta^{13}\text{C}$  of  
360 the biomass (Fig. 4A), presumably reflects the downstream consequence of an upstream change  
361 in  $\delta^{13}\text{C}$  of the metabolic substrate taken up and ultimately respired. However, the more negative  
362  $\delta^{13}\text{C}$  of respired CO<sub>2</sub> compared to that of biomass is, to our knowledge, the most direct evidence  
363 to date for <sup>13</sup>C discrimination during respiration of a heterotrophic microbe. The observation of a  
364 substantial respiratory <sup>13</sup>C discrimination corroborates inferences drawn in earlier studies  
365 (Šantrůčková et al., 2000; Fernandez and Cadisch, 2003) and is also consistent with plant studies  
366 reporting C isotope discrimination during dark respiration in roots (Klumpp et al., 2005;  
367 Bathellier et al., 2009; Ghashghaie and Badeck, 2014). Our observations of respiratory  
368 discrimination against <sup>13</sup>C highlight the similarity of heterotrophic, aerobic respiratory pathways,  
369 and isotope effects within them, across life's domains.

370 In contrast to the discontinuous relationship between biomass  $\delta^{13}\text{C}$  and temperature, we observed  
371 a comparably continuous and linear increase in respiratory discrimination against  $^{13}\text{C}$  with  
372 temperature (Fig. 4B). This increase generated a marginally positive significant ( $P=0.08$ )  
373 correlation with SRR (Fig. 6), and hence a marginally significant ( $P=0.07$ ) correlation with CUE.  
374 A physiological interpretation of this finding is not straightforward, as multiple, possibly  
375 simultaneous enzymatic fractionations may have contributed to the observed  $\delta^{13}\text{C}$  of respired  
376  $\text{CO}_2$  (Dijkstra et al., 2011; Tcherkez et al., 2012). It could simply result from a proportionally  
377 increasing flux through respiratory pathways, with associated stronger expression of  $^{13}\text{C}$   
378 discrimination by the enzymes involved (Tcherkez et al., 2012), or could result from increasing  
379 temperatures altering the relative fluxes through respiratory pathways (Chung et al., 1976;  
380 Wittmann et al., 2007; Dijkstra et al., 2011) such that the overall observed respiratory  $^{13}\text{C}$   
381 discrimination increased with temperature. This may be possible given that respiratory pathways  
382 can exhibit distinct fractionation factors (Bathellier et al., 2009 and references therein) and  
383 prompt different, specific C atoms to undergo decarboxylation from the two glucose units of the  
384 substrate cellobiose, which contain non-randomly distributed  $^{13}\text{C}$  atoms (Rossmann et al., 1991;  
385 Gleixner and Schmidt, 1997). If relative fluxes through different respiratory pathways changed  
386 with temperature, the continuous nature of the relationship between temperature and respiratory  
387  $^{13}\text{C}$  discrimination suggests a smooth transition compared to the abrupt and discontinuous shifts  
388 in apparent uptake and/or secretion discrimination described above. Future metabolic flux  
389 analyses linked to isotopic approaches sensitive enough to quantify C isotopes in microbial  
390 exudation will be well-suited to explore how C allocation to distinct, aerobic respiratory  
391 pathways may vary with temperature and result in varying  $\delta^{13}\text{C}$  of respired  $\text{CO}_2$ .

392

#### 393 **4. Conclusions**

394 Our observations clearly show a decline in microbial CUE with increasing temperature when C  
395 substrate is plentiful and demonstrate the mechanism driving it – an increase in SRR. The  
396 relationship between CUE and temperature underscores the importance of incorporating variable,  
397 temperature dependent SRR, which influences CUE and growth efficiency, in ecosystem process  
398 models. The temperature-driven changes in SRR and respiratory discrimination against  $^{13}\text{C}$  were  
399 not independent of each other, suggesting that increasing SRR, to some degree, drives enhanced  
400 C isotopic discrimination. We demonstrate that C isotope discrimination associated with  
401 microbial decomposition of OM can impart large and variable isotopic signatures on C pools  
402 typically characterized and interpreted in biogeochemical studies at any scale. Further  
403 exploration of the drivers of C isotope fractionations during microbial OM transformations could  
404 exploit an experimental approach similar to that presented here to investigate the roles of  
405 resource stoichiometry, identity of the organism or the supplied substrate, or competition among  
406 microbial populations. To date, efforts to partition flux components of net ecosystem exchange  
407 have assumed little to no fractionation between respired substrates and the resultant  $\text{CO}_2$ . Our  
408 results suggest that this assumption must be reevaluated, and represent a first step towards an  
409 isotopically explicit, mechanistic framework for microbial C isotope fluxes in Earth system  
410 models.

411

412 **Author contribution:**

413 C.A.L. and K.M. performed the experiments; all authors contributed to all other parts and stages  
414 of the manuscript.

415

416 **Data availability:** The data presented in this study are available for collaborative use by anyone  
417 interested; contact the corresponding author for access to the data.

418

419 **Acknowledgements:**

420 We thank Dr. Susan Ziegler, Dr. Jarad Mellard and Chao Song for helpful discussions during the  
421 design of the experiments, Greg Caine for expert stable isotope analysis and the provision of  
422 isotopic standards, Drs. Susan Ziegler, Mike Burrell, Karl Auerswald, Hanns-Ludwig Schmidt  
423 and John Kelly for comments on the manuscript, Gil Ortiz with assistance generating Figure 5,  
424 anonymous referees for their time and constructive comments, and the National Science  
425 Foundation of the USA for funding (grant no. DEB-0950095 and EAR-1331846).

426

427 **References:**

428 Abraham, W.-R., Hesse, C., and Pelz, O.: Ratios of carbon isotopes in microbial lipids as an  
429 indicator of substrate usage, *App. Environ. Microbiol.*, 64, 4202-4209, 1998.

430 Allison, S.D., Wallenstein, M.D., and Bradford, M.A.: Soil-carbon response to warming  
431 dependent on microbial physiology, *Nat. Geosci.*, 3, 336-340, 2010.

432 Apple, J.K., del Giorgio, P.A., and Kemp, W.M.: Temperature regulation of bacterial production,  
433 respiration, and growth efficiency in a temperate salt-marsh estuary, *Aquat. Microb. Ecol.*, 43,  
434 243-254, 2006.

435 Barbosa, Î.C.R., Köhler, I.H., Auerswald, K., Lüps, P., and Schnyder, H.: Last-century changes of  
436 alpine grassland water-use efficiency: a reconstruction through carbon isotope analysis of a time-  
437 series of *Capra ibex* horns, *Glob. Change Biol.*, 16, 1171-1180, 2010.

438 Bathellier, C., Tcherkez, G., Blligny, R., Gout, E., Cornic, G., and Ghashghaie, J.: Metabolic  
439 origin of the  $\delta^{13}\text{C}$  of respired  $\text{CO}_2$  in roots of *Phaseolus vulgaris*, *New Phytol.*, 181, 387-399,  
440 2009.

441 Billings, S.: Soil organic matter dynamics and land use change at a grassland/forest ecotone, *Soil*  
442 *Biol. Biochem.*, 38, 2934-2943, 2006.

443 Blair, N., Leu, A., Muñoz, E., Olsen, J., Kwong, E., and Des Marais, D.: Carbon isotopic  
444 fractionation in heterotrophic microbial metabolism, *Appl. Environ. Microbiol.*, 50, 996-1001,  
445 1985.

446 Bowling, D.R., Pataki, D.E., and Randerson, J.T.: Carbon isotopes in terrestrial ecosystem pools  
447 and  $\text{CO}_2$  fluxes, *New Phytol.*, 178, 24-40, 2008.

448 Brüggemann, N., Gessler, A., Kayler, Z., Keel, S.G., Badeck, F., Barthel, M., Boeckx, P.,  
449 Buchmann, N., Brugnoli, E., Esperschütz, J., Gavrichkova, O., Ghashghaie, J., Gomez-  
450 Casanovas, N., Keitel, C., Knohl, A., Kuptz, D., Palacio, S., Salmon, Y., Uchida, Y., and Bahn,  
451 M.: Carbon allocation and carbon isotope fluxes in the plant-soil-atmosphere continuum: a  
452 review, *Biogeosci.*, 8, 3457-3489, 2011.

453 Bull, A.T.: The renaissance of continuous culture in the post-genomics age, J. Ind. Microbiol.  
454 Biotechnol., 37, 993-1021, 2010.

455 Chrzanowski, T.H., and Grover J.P.: Element content of *Pseudomonas fluorescens* varies with  
456 growth rate and temperature: A replicated chemostat study addressing ecological stoichiometry,  
457 Limnol. Oceanogr., 53, 1242-1251, 2008.

458 Chung, B.H., Cannon, R.Y., and Smith, R.C.: Influence of growth temperature on glucose  
459 metabolism of a psychrotrophic strain of *Bacillus cereus*, Appl. Environ. Microb., 31, 39-45,  
460 1976.

461 Cleland, W.W.: The use of isotope effects to determine enzyme mechanisms, Arch. Biochem.  
462 Biophys., 433, 2-12, 2005.

463 Cole, J.J., Findlay, S., and Pace M.L.: Bacterial production in fresh and saltwater ecosystems: a  
464 cross-system overview, Mar. Ecol. Prog. Ser., 43, 1-10, 1988.

465 Cotner, J.B., and Biddanda, B.A.: Small players, large role: microbial influence on  
466 biogeochemical processes in pelagic aquatic ecosystems, Ecosystems, 5, 105-121, 2002.

467 Cotner, J.B., Makino, W., and Biddanda, B.A.: Temperature affects stoichiometry and  
468 biochemical composition of *Escherichia coli*, Microb. Ecol., 52, 26-33, 2006.

469 Craig, H., and Gordon, L.I.: Deuterium and 18 oxygen variations in the ocean and the marine  
470 atmosphere. In: Proceedings of a conference on stable isotopes in oceanographic studies and  
471 paleotemperatures. Ed: E. Tongioli, Lischi & Figli, Pisa, 1965.

472 Dawson, P.S.S.: Microbial growth, Dowden, Hutchinson & Ross, Stroudsburg, 1974.

473 del Giorgio, P.A., and Cole, J.J.: Bacterial growth efficiency in natural aquatic systems, *Annu.*  
474 *Rev. Ecol. Syst.*, 29, 503-541, 1998.

475 Dijkstra, F.A., Hobbie, S.E., Knops, J.M.H., and Reich, P.B.: Nitrogen stabilization and plant  
476 species interact to influence soil carbon stabilization, *Ecol. Lett.*, 7, 1192-1198, 2004.

477 Dijkstra, P., Thomas, S.C., Heinrich, P.L., Koch, G.W., Schwartz, E., and Hungate, B.A.: Effect  
478 of temperature on metabolic activity of intact microbial communities: evidence for altered  
479 metabolic pathway activity but not for increased maintenance respiration and reduced carbon use  
480 efficiency, *Soil Biol. Biochem.*, 43, 2023-2031, 2011.

481 Egli, T.: Microbial growth and physiology: a call for better craftsmanship, *Front. Microbiol.*,  
482 6:287, DOI: 10.3389/fmicb.2015.00287, 2015.

483 El-Mansi, E.M.T., Holms, W.H.: Control of carbon flux to acetate excretion during growth of  
484 *Escherichia coli* in batch and continuous cultures, *J. General Microbiol.*, 135, 2875-883, 1989.

485 Farquhar, G.D., O'Leary, M.H., and Berry, J.A.: On the relationship between carbon isotope  
486 discrimination and the intercellular carbon dioxide concentration in leaves, *Aust. J. Plant*  
487 *Physiol.*, 9, 121-137, 1982.

488 Farquhar, G.D., and Richards, R.A.: Isotopic composition of plant carbon correlates with water-  
489 use efficiency of wheat genotypes, *Aust. J. Plant Physiol.*, 11, 539-552, 1984.

490 Ferenci, T.: Bacterial physiology, regulation and mutational adaptation in a chemostat  
491 environment, *Adv. Microb. Physiol.*, 53, 169-230, 2008.

492 Fernandez, I., and Cadisch, G.: Discrimination against  $^{13}\text{C}$  during degradation of simple and  
493 complex substrates by two white rot fungi, *Rapid Commun. Mass Spectrom.*, 17, 2614-2620,  
494 2003.

495 Frey, S., Lee, J., Melillo, J.M., and Six, J.: The temperature response of soil microbial efficiency  
496 and its feedback to climate, *Nat. Clim. Change*, 3, 395-398, 2013.

497 Fry, B.: *Stable Isotope Ecology*, Springer, New York, 2006.

498 Gamnitzer, U., Moyes, A.B., Bowling, D.R., and Schnyder, H.: Measuring and modeling the  
499 isotopic composition of soil respiration: insights from a grassland tracer experiment, *Biogeosci.*,  
500 8, 333-1350, 2011.

501 Ghashghaie, J., and Badeck, F.W.: Opposite carbon isotope discrimination during dark  
502 respiration in leaves versus roots – a review, *New Phytol.*, 201, 751-769.

503 Gillooly, J.F., Brown, J.H., West, G.B., Savage, V.M., and Charnov, E.L.: Effects of size and  
504 temperature on metabolic rate, *Science*, 293, 2248-2251, 2001.

505 Gleixner, G., and Schmidt H.-L.: Carbon isotope effects on the Fructose-1,6-bisphosphate  
506 aldolase reaction, origin for non-statistical  $^{13}\text{C}$  distributions in carbohydrates, *J. Biol. Chem.*,  
507 272, 5382-5387, 1997.

508 Goldman, J.C., and Dennet, M.R.: Growth of marine bacteria in batch and continuous culture  
509 under carbon and nitrogen limitation, *Limnol. Oceanogr.*, 45, 789-800, 2000.



510 Hall, E.K., Neuhauser, C., and Cotner, J.B.: Toward a mechanistic understanding of how natural  
511 bacterial communities respond to changes in temperature in aquatic ecosystems. *ISME J*, 2, 471-  
512 481, 2008.

513 Hanson, P.J., Edwards, N.T., Garten, C.T., and Andrews, J.A.: Separating root and microbial  
514 contributions to soil respiration: a review of methods and observations. *Biogeochem.*, 48, 115-  
515 146, 2000.

516 Hedges, J.I., Eglinton, G., Hatcher, P.G., Kirchman, D.L., Arnosti, C., Derenne, S., Evershed,  
517 R.P., Kögel-Knabner, I., de Leeuw, J.W., Littke, R., Michaelis, W., Rullkötter, J.: The  
518 molecularly-uncharacterized component of nonliving organic matter in natural environments,  
519 *Org. Geochem.*, 31, 945-958, 2000.

520 Hobbie, J.E., and Hobbie, E.A.: Microbes in nature are limited by carbon and energy: the  
521 starving-survival lifestyle in soil and consequences for estimating microbial rates, *Front.*  
522 *Microbiol.*, 4, doi: 10.3389/fmicb.2013.00324, 2013.

523 Kayser, A., Weber, J., Hecht, V., and Rinas, U.: Metabolic flux analysis of *Escherichia coli* in  
524 glucose-limited continuous culture. I. Growth-rate dependent metabolic efficiency at steady-  
525 state, *Microbiol.*, 151, 693-706, 2005.

526 Kirschbaum, M.U.F.: The temperature-dependence of organic-matter decomposition – still a  
527 topic of debate, *Soil Biol. Biochem.*, 38, 2510-2518, 2006.

528 Klumpp, K., Schäufele, R., Lötscher, M., Lattanzi, F.A., Feneis, W., and Schnyder, H.: C-isotope  
529 composition of CO<sub>2</sub> respired by shoots and roots: fractionation during dark respiration?, *Plant*  
530 *Cell Environ.*, 28, 241-250, 2005.

531 Kucera, C.L., and Kirkham, D.R.: Soil respiration studies in tallgrass prairie in Missouri,  
532 Ecology, 52, 912-915, 1971.

533 Lehmeier, C.A., Min, K., Niehues, N.D., Ballantyne, F.IV., and Billings, S.A.: Temperature-  
534 mediated changes of exoenzyme-substrate reaction rates and their consequences for the carbon to  
535 nitrogen flow ration of liberated resources, Soil Biol. Biochem., 57, 374-382, 2013.

536 Manzoni, S., Taylor, P., Richter, A., Porporato, A., and Ågren, G.I.: Environmental and  
537 stoichiometric controls on microbial carbon-use efficiency in soils, New Phytol., 196, 79-91,  
538 2012.

539 Min, K., Lehmeier, C.A., Ballantyne, F., Tatarko, A., and Billings, S.A.: Differential effects of  
540 pH on temperature sensitivity of organic carbon and nitrogen decay, Soil Biol. Biochem., 76,  
541 193-200, 2014.

542 Mook, W.G., Bommerson, J.C., and Staverman, W.H.: Carbon isotope fractionation between  
543 dissolved bicarbonate and gaseous carbon dioxide, Earth Planet. Sci. Lett., 22, 169-176, 1974.

544 Nanchen, A., Schicker A., and Sauer U.: Nonlinear dependency of intracellular fluxes on growth  
545 rate in miniaturized continuous cultures of *Escherichia coli*, Appl. Environ. Microb., 73, 1164-  
546 1172, 2006.

547 Nickerson, N., Egan, J., and Risk, D.: Iso-FD: A novel method for measuring the isotopic  
548 signature of surface flux, Soil Biol. Biochem., 62, 99-106, 2013.

549 O'Leary, M.H.: Carbon isotope fractionation in plants, Phytochem., 20, 553-567, 1981.

550 Park, R., and Epstein, S.: Metabolic fractionation of  $C^{13}$  &  $C^{12}$  in plants, *Plant Physiol.*, 36, 133-  
551 138, 1961.

552 Pataki, D.E., Ehleringer, J.E., Flanagan, L.B., Yakir, D., Bowling, D.R., Still, C.J., Buchmann,  
553 N., Kaplan, J.O., and Berry, J.A.: The application and interpretation of Keeling plots in terrestrial  
554 carbon cycle research, *Glob. Biogeochem. Cycles*, 17, doi:10.1029/2001GB001850, 2003.

555 Pomeroy, L.R., and Wiebe, W.J.: Temperature and substrate as interactive limiting factors for  
556 marine heterotrophic bacteria, *Aquat. Microb. Ecol.*, 23, 187-204, 2001.

557 Rivkin, R.B., and Legendre, L.: Biogenic carbon cycling in the upper ocean: effects of microbial  
558 respiration, *Science*, 291, 2398-2400, 2001.

559 Rossmann, A., Butzenlechner, M., and Schmidt, H.L.: Evidence for a nonstatistical carbon  
560 isotope distribution in natural glucose, *Plant Physiol.*, 96, 609-614, 1991.

561 Šantrůčková, H., Bird, M.I., and Lloyd, J.: Microbial processes and carbon-isotope fractionation  
562 in tropical and temperate grassland soils, *Funct. Ecol.*, 14, 108-114, 2000.

563 Schimel, D.S.: Terrestrial ecosystems and the carbon-cycle, *Glob. Change Biol.*, 1, 77-91, 1995.

564 Smith, H.L., and Waltman, P.E.: The theory of the chemostat: dynamics of microbial  
565 competition, Cambridge University Press, New York, 1995.

566 Stumm, W., and Morgan, J.J.: *Aquatic Chemistry: An introduction emphasizing chemical*  
567 *equilibria in natural waters*, John Wiley & Sons, New York, 1981.

568 Subke, J.-A., Inglima, I., and Cotrufo, M.F.: Trends and methodological impacts in soil  $CO_2$  flux  
569 partitioning: A metaanalytical review, *Glob. Change Biol.*, 12, 921-943, 2006.

570 Szaran, J.: Achievement of carbon isotope equilibrium in the system  $\text{HCO}_3^-$  (solution) –  $\text{CO}_2$   
571 (gas). *Chem. Geol.*, 142, 79-86, 1997.

572 Tcherkez, G., Mahé, A., and Hodges, M.:  $^{12}\text{C}/^{13}\text{C}$  fractionations in plant primary metabolism,  
573 *Trends Plant Sci.*, 16, 499-506, 2012.

574 Tempest, D.W., and Neijssel, O.M.: Eco-physiological aspects of microbial growth in aerobic  
575 nutrient-limited environments, *Adv. Microb. Ecol.*, 2, 105-153, 1978.

576 Trumbore, S.: Carbon respired by terrestrial ecosystems – recent progress and challenges, *Glob.*  
577 *Change Biol.*, 12, 141-153, 2006.

578 Tucker, C.L., Bell, J., Pendall, E., and Ogle, K.: Does declining carbon-use efficiency explain  
579 thermal acclimation of soil respiration with warming?, *Glob. Change Biol.*, 19, 252-263, 2013.

580 Vogel, J.C., Grootes, P.M., and Mook, W.G.: Isotopic fractionation between gaseous and  
581 dissolved carbon dioxide, *Z. Physik*, 230, 225-238, 1970.

582 Werner, C., and Gessler, A.: Diel variations in the carbon isotope composition of respired  $\text{CO}_2$   
583 and associated carbon sources: a review of dynamics and mechanisms, *Biogeosci.*, 8, 2437-2459,  
584 2011.

585 Werner, R.A., Buchmann, N., Siegwolf, R.T.W., Kornexl, B.E., and Gessler, A.: Metabolic  
586 fluxes, carbon isotope fractionation and respiration – lessons to be learned from plant  
587 biochemistry, *New Phytol.*, 191, 10-15, 2011.

588 Werth, M., and Kuzyakov, Y.:  $^{13}\text{C}$  fractionation at the root-microorganisms-soil interface: a  
589 review and outlook for partitioning studies, *Soil Biol. Biochem.*, 42, 1372-1384, 2010.

590 Wieder, W.R., Bonan, G.B., and Allison, S.D.: Global soil carbon projections are improved by  
591 modelling microbial processes, *Nat. Clim. Change*, 3, 909-912, 2013.

592 Wittmann, C., Weber, J., Betiku, E., Krömer, J., Böhm, D., and Rinas, U.: Response of fluxome  
593 and metabolome to temperature-induced recombinant protein synthesis in *Escherichia coli*, *J.*  
594 *Biotechnol.*, 132, 375-384, 2007.

595

596

597

598

599

600

601

602

603

604

605

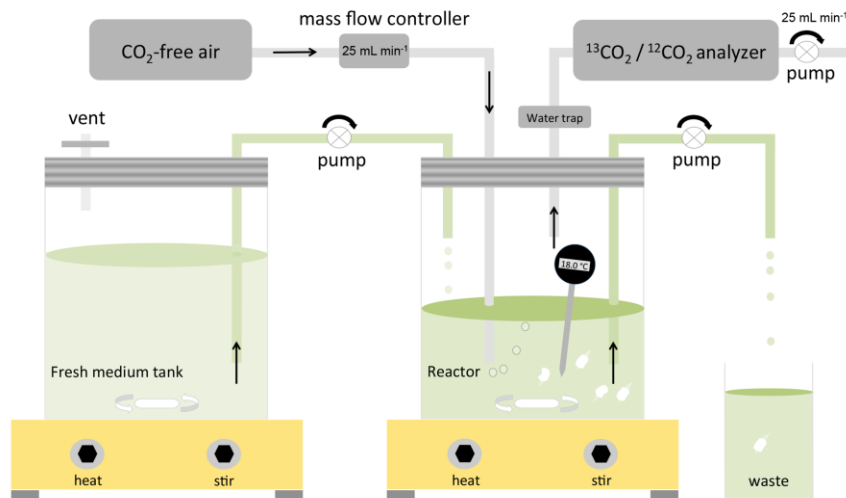
606

607

608 **Figures:**

609 **Fig. 1.** Chemostat system comprised of *P. fluorescens* growing on cellobiose. Seven independent  
610 experiments were conducted, with reactor temperatures of 13, 14.5, 16, 18, 21, 23.5 and 26.5 °C;  
611 all other conditions were identical. During continuous flow, dilution rate of the reactor  
612 (mean=0.137±0.01 h<sup>-1</sup> across all experiments) equals microbial growth rate. A peristaltic pump  
613 supplied fresh nutrient medium from a reservoir tank to the reactor and removed reactor medium  
614 (including biomass) at a constant rate. Headspace volume was flushed with CO<sub>2</sub>-free air,  
615 bubbling through reactor medium and supplying microorganisms with O<sub>2</sub>. A <sup>13</sup>CO<sub>2</sub>/<sup>12</sup>CO<sub>2</sub>  
616 analyzer continuously sampled reactor headspace and measured the concentration and δ<sup>13</sup>C of  
617 respired CO<sub>2</sub>.

618

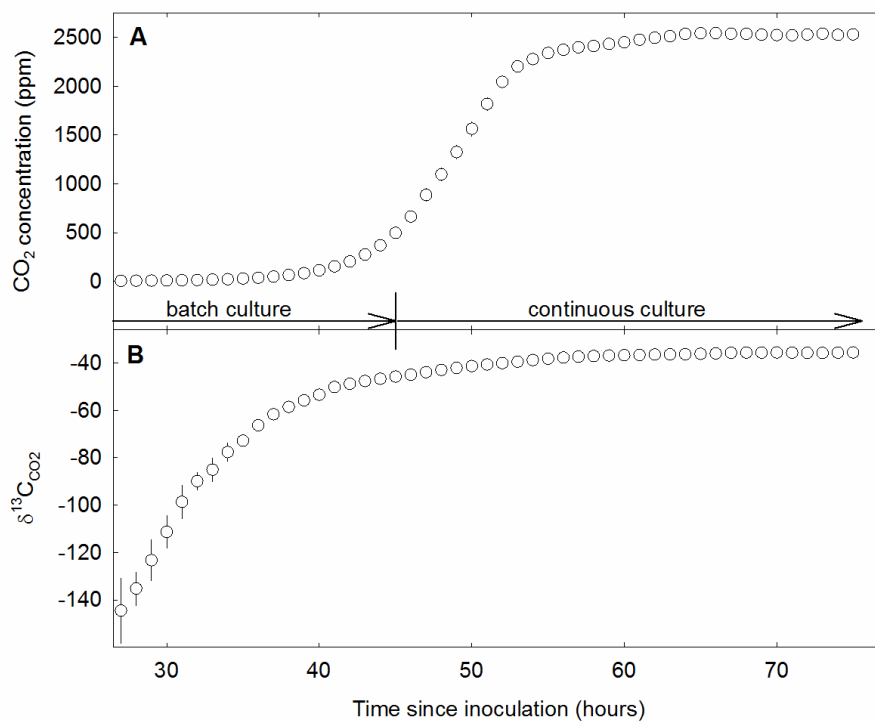


619

620

621 **Fig. 2.** Example time course of the evolution of reactor headspace CO<sub>2</sub> concentration (A) and  
622  $\delta^{13}\text{C}$  of the CO<sub>2</sub> (B) of the chemostat run at 23.5 °C in hours since inoculation of the reactor with  
623 pre-cultured *P. fluorescens*. Data points are hourly means. Error bars (where visible) denote  $\pm 1$   
624 SD. The reactor was shifted from batch to continuous culture mode 45 h after inoculation.  
625 Microbial respiration rate and the  $\delta^{13}\text{C}$  of respired CO<sub>2</sub> were measured between 70 and 74 h after  
626 inoculation when the culture reached steady-state.

627

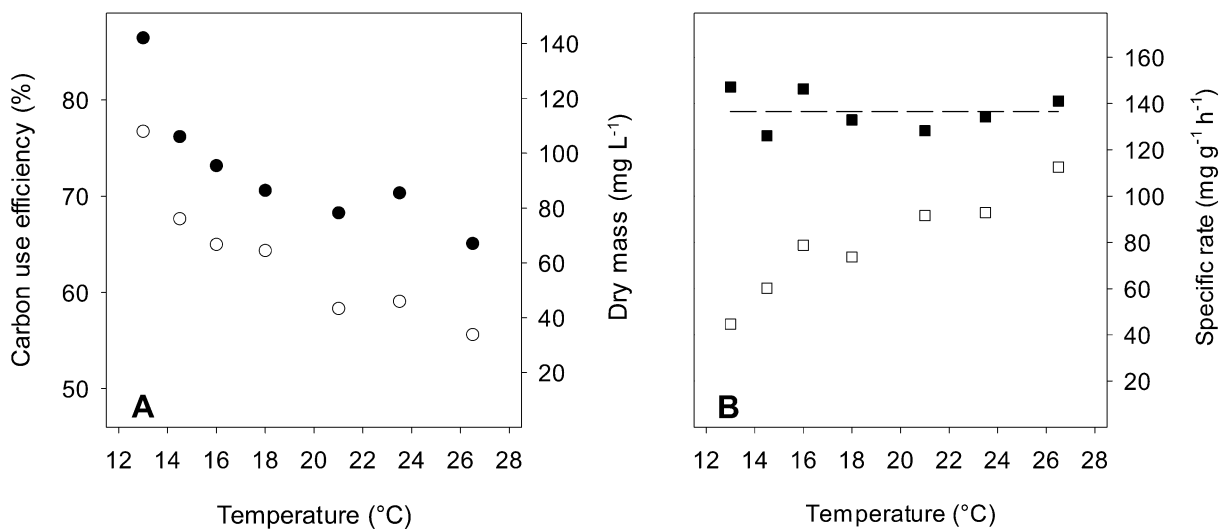


628

629

630 **Fig. 3.** Steady-state process variables of *P. fluorescens* growing in chemostats at specified  
 631 temperatures. Microbial carbon use efficiency (○; A), dry microbial biomass (●; A); specific  
 632 growth rate (■; B), and specific respiration rate (□; B), expressed in mg C per g of microbial  
 633 biomass-C and hour. The dashed line denotes the average of the seven specific growth rates  
 634 ( $137 \text{ mg g}^{-1} \text{ h}^{-1}$ ).

635



636

637

638

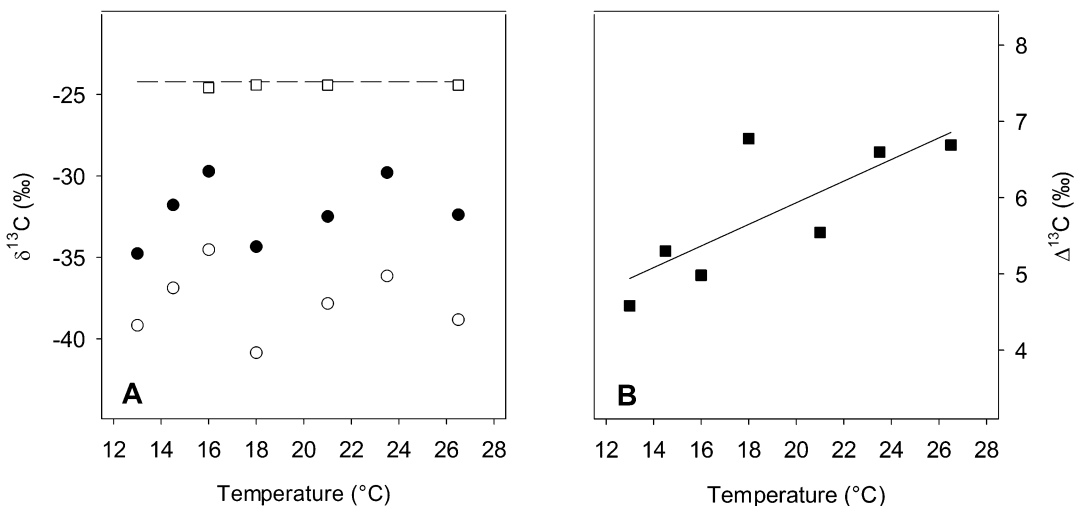
639

640



641 **Fig. 4.** Steady-state  $\delta^{13}\text{C}$  of microbial biomass ( $\bullet$ ; A) and of respired  $\text{CO}_2$  ( $\circ$ ; A), and C isotope  
642 discrimination during respiration ( $\Delta^{13}\text{C}$ ; B) of *P. fluorescens* growing in chemostats at specified  
643 temperatures. In panel A, the dashed line denotes the  $\delta^{13}\text{C}$  of the substrate cellobiose (-24.2‰),  
644 and  $\delta^{13}\text{C}$  of reactor filtrate is shown as open squares; standard errors, derived from multiple  
645 measurements across time during steady-state, are smaller than the size of the symbols.  $\Delta^{13}\text{C}$  is  
646 calculated as  $\Delta^{13}\text{C} = (\delta^{13}\text{C}_{\text{biomass}} - \delta^{13}\text{C}_{\text{respired CO}_2}) / (1 + \delta^{13}\text{C}_{\text{respired CO}_2})$ . The solid line denotes  
647 linear regression of  $\Delta^{13}\text{C}$  vs. temperature ( $y = 0.14x + 3.1$ ;  $R^2 = 0.61$ ;  $P=0.04$ ).

648



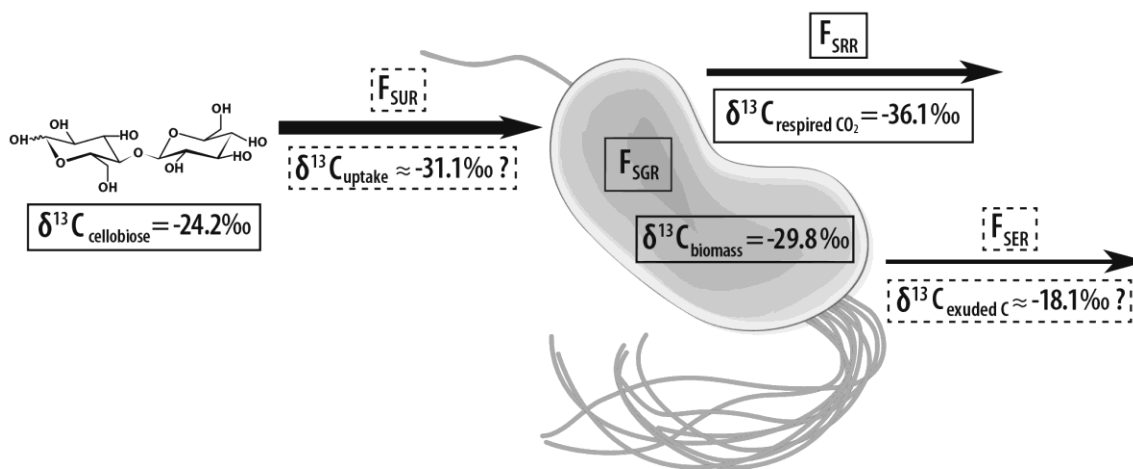
649

650

651

652

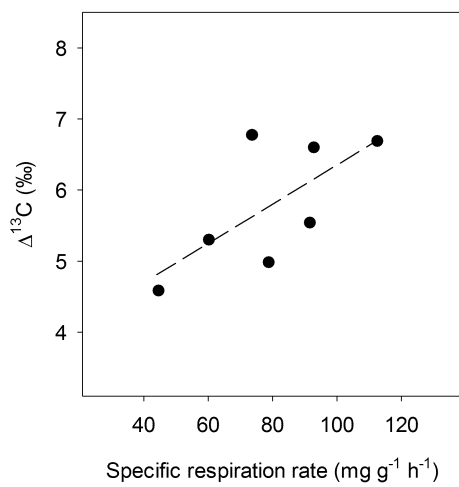
653 **Fig. 5.** Schematic of an individual *P. fluorescens* cell, representing the sample population  
 654 growing at 23.5 °C with one available substrate at a constant relative growth rate of 0.14 h<sup>-1</sup> at  
 655 steady-state (Fig. 2), with measured (solid boxed) and estimated (dashed boxed) magnitudes of C  
 656 and <sup>13</sup>C fluxes into and out of the population. Designated fluxes include specific uptake rate of  
 657 cellobiose (F<sub>SUR</sub>), specific growth rate (F<sub>SGR</sub>), specific respiration rate (F<sub>SRR</sub>) and specific  
 658 excretion rate (F<sub>SER</sub>), in relation to steady-state biomass-C in the chemostat, where F<sub>SUR</sub> = F<sub>SGR</sub> +  
 659 F<sub>SRR</sub> + F<sub>SER</sub>. The estimate of δ<sup>13</sup>C<sub>uptake</sub> is based on the assumption that δ<sup>13</sup>C<sub>exuded C</sub> is 11.7‰ less  
 660 negative than δ<sup>13</sup>C<sub>biomass</sub> (Blair et al., 1985) and that F<sub>SER</sub> is 10% of the sum of F<sub>SGR</sub> and F<sub>SRR</sub> (El-  
 661 Mansi and Holms, 1989). In contrast to this experimental system, in natural environments  
 662 measurements of boxed pools and fluxes can be confounded by the presence of dormant  
 663 microorganisms, unknown microbial growth rates, diverse available substrates, and a lack of  
 664 steady-state CO<sub>2</sub> fluxes.



667

668 **Fig. 6.** Correlation between the specific respiration rate (in mg C per g microbial biomass-C and  
669 hour) of *P. fluorescens* growing in continuous chemostat culture at temperatures ranging from 13  
670 °C to 26.5 °C and the carbon isotope discrimination during respiration. The dashed line denotes  
671 a linear regression of the form  $y = 0.03x + 3.6$ ;  $R^2 = 0.48$ ;  $P=0.08$ .

672



673